Evidence for shape coexistence and superdeformation in ^{24}Mg

J.T.H. Dowie [a,*], T. Kibédi [a], D.G. Jenkins [b,c], A.E. Stuchbery [a], A. Akber [a], H.A. Alshammari [a], N. Aoi [d], A. Avaa [e,f], L.J. Bignell [a], M.V. Chisapi [e,g], B.J. Coombes [a], T.K. Eriksen [a,1], M.S.M. Gerathy [a], T.J. Gray [a], T.H. Hoang [d], E. Ideguchi [d], P. Jones [e], M. Kumar Raju [d], G.J. Lane [a], B.P. McCormick [a], L.J. McKie [a], A.J. Mitchell [a], N.J. Spinks [a], B.P.E. Tee [a]

[a] Department of Nuclear Physics, Research School of Physics, Australian National University, Canberra, ACT 2601, Australia
[b] Department of Physics, University of York, York YO10 5DD, UK
[c] University of Strasbourg Institute of Advanced Studies (USIAS), Strasbourg, France
[d] Research Center for Nuclear Physics (RCNP), 10-1 Mihogaoka, Ibaraki, Osaka, 567-0047, Japan
[e] Department of Subatomic Physics, iThemba LABS, P.O. Box 722, Somerset West 7129, South Africa
[f] School of Physics, University of the Witwatersrand, Johannesburg, 2000, South Africa
[g] Department of Physics, Faculty of Science, Stellenbosch University, Private Bag X1, Matieland 7602, Stellenbosch, South Africa

ARTICLE INFO

ABSTRACT

The $E0$ transition depopulating the first-excited 0^+ state in ^{24}Mg has been observed for the first time, and the $E0$ transition strength determined by electron-positron pair and γ-ray spectroscopy measurements performed using the Super-e pair spectrometer. The $E0$ transition strength is $\rho^2 \times 10^3 = 380(70)$. A two-state mixing model implies a deformation of the first-excited 0^+ state of $\beta_2 \approx 1$ and a change in the mean-square charge radius of $\Delta\langle r^2 \rangle \approx 1.9$ fm^2, which suggests a significant shape change between the ground state and first-excited 0^+ state in ^{24}Mg. The observed $E0$ strength gives direct evidence of shape coexistence and superdeformation in ^{24}Mg, bringing this nucleus into line with similar behaviour in nearby $N = Z$ nuclei. This result agrees with recent theoretical work on the cluster nature of ^{24}Mg and has potential ramifications for nuclear reactions of astrophysical importance.

© 2020 The Author(s). Published by Elsevier B.V. This is an open access article under the CC BY license (http://creativecommons.org/licenses/by/4.0/). Funded by SCOAP^3.

1. Introduction

Shape coexistence is a phenomenon whereby an atomic nucleus will display different nuclear shapes at relatively low excitation energy. It appears to be a fundamental property of the nuclear quantum many-body system, having been observed in many different regions of the nuclear chart [1]. The most extreme nuclear shape observed in bound nuclei is called superdeformation, wherein the nucleus has an elongated spheroidal shape with a 2:1 axis ratio. Hyperdeformation — a 3:1 axis ratio — is predicted to occur in nuclei but has not been experimentally observed [2]. In light, α-conjugate nuclei, those whose proton and neutron numbers are an integer number of α-particles, superdeformation appears to be related to the clustering of the nucleons into an assembly of α-particles. This structure can have significant implications for nuclear reaction outcomes [1,3–5], especially those relevant to nuclear astrophysics such as the resonances in the triple-α reaction in the creation of ^{12}C [3–7].

In even-even nuclei, the properties of low-lying 0^+ states play a pivotal role in understanding shape coexistence [1]. In light, α-conjugate nuclei, the 0^+ states can be bandheads of rotating strongly-deformed cluster configurations [3]. The famous example is in ^{12}C where the first-excited 0^+ state — the Hoyle state at 7.65 MeV — is strongly deformed and is considered to be an ensemble of three α-particles [6–9]. In ^{16}O and ^{40}Ca, both doubly-magic nuclei, the low-lying excited 0^+ states can be described as arising from multi-particle/multi-hole configurations (4p-4h, 8p-8h), natural analogs to excited α-particle configurations [1,3,10–12].

^{24}Mg is an α-conjugate nucleus ($Z = 12$, $N = 12$) and is of astrophysical interest for its role in stellar nucleosynthesis. It is involved in a number of important exothermic heavy-ion reactions: ^{24}Mg acts as a source of neutrons in Ne burning, a source of α-particles in O and Si burning, and as both an intermedi-
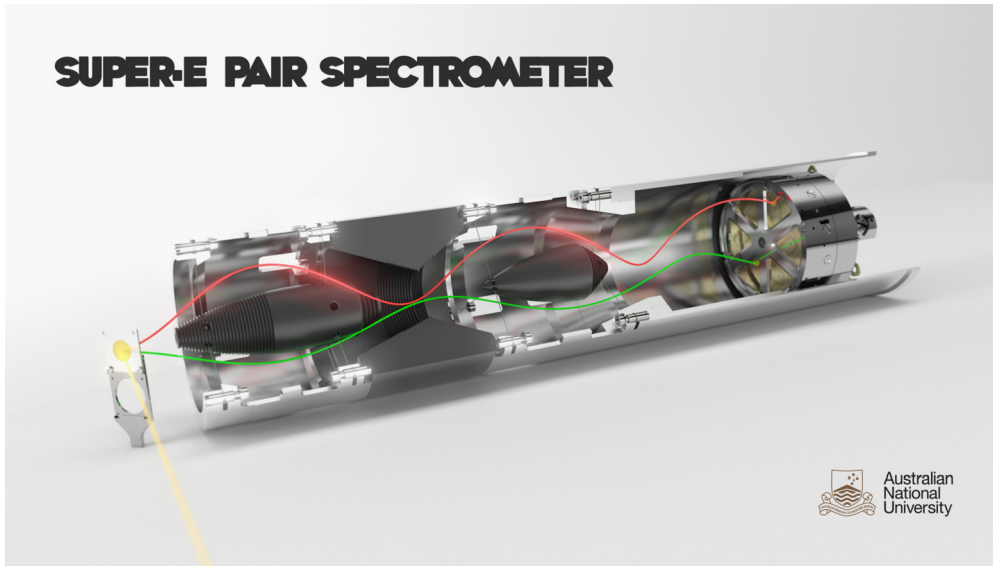
Fig. 1. A cut-away, rendered image of the Super-e pair spectrometer. In dark grey down the centre of the bore are the *HeavyMet* baffles, and around the bore are the superconducting coils — not pictured. The target is positioned on the left and the *Miel* detector array on the right. In red and green (colour only) lines are schematic traces of the trajectories of the electron-positron pairs emitted from the target that lie within the acceptance window.

ary and final product of ^{12}C+^{12}C reactions [13]. ^{24}Mg has several high-energy 0^+ states which have been suggested to be α-cluster configurations and the heads of rotational bands, based on a number of different calculations using a ^{12}C+^{12}C model [14], along with α+^{20}Ne and $\alpha + \alpha$+^{16}O models [15,16]. Clustering in ^{24}Mg has important implications for astrophysical reactions, especially for those involving the ^{12}C+^{12}C cross-section, which appears to be dominated by resonances [2,5,17–21]. ^{24}Mg is predicted to form both super- and hyper-deformed states due to alpha-clustering [2].

Electric monopole ($E0$) transitions, the only significant decay mode between $J^{\pi} = 0^+$ states (excluding two-quantum processes), provide a unique probe into nuclear structure. The nuclear $E0$ transition strength, $\rho^2(E0)$, is large when there is a sizable change in the nuclear mean-square charge radius, and when there is also strong mixing between the parent configurations of different deformation [4]. $E0$ transitions are then a direct experimental tool to investigate the change in deformation between two nuclear states with different deformation as well as being sensitive to the degree of mixing between the two states.

In this article we report the first observation and measurement of the $E0$ transition from the 6.432-MeV first-excited 0^+ state to the ground state in ^{24}Mg. This E0 transition has not been observed to date [22]. The magnitude of the monopole matrix element — $M(E0)$ — has been measured in a model-dependent fashion by inelastic electron scattering [23–25]. The current adopted value for $\rho^2(E0)$ is large: 288(11) milliunits; this value far exceeds simple shell-model estimates of $E0$ strengths in the sd shell [3,4]. A significant change in the mean-square charge radius of the nucleus between the first-excited 0^+ state and the ground state along with mixing is therefore suggested. Theoretical work has proposed that the excited 0^+ state is a mixture of the mean-field configuration and the α+Ne cluster configuration [16]. A model independent evaluation of the $E0$ strength to confirm the very large $E0$ strength and thereby test the α-cluster picture of ^{24}Mg is warranted.

2. Experiment

The experiment was carried out at the Heavy Ion Accelerator Facility (HIAF) at the Australian National University (ANU) using the superconducting electron spectrometer (Super-e) [26] to perform the electron-positron pair and γ-ray measurements. The Super-e is a superconducting magnetic-lens spectrometer for the

measurement of conversion electrons and electron-positron pairs with excellent background suppression [26,27]. It consists of a Si(Li) detector array — named *Miel*, consisting of 6 Si(Li) detectors, each 9-mm thick — a superconducting solenoid, and central *HeavyMet* baffles. An image of the Super-e rendered from the engineering drawings is shown in Fig. 1. A passively shielded HPGe detector is placed 144 cm from the target to measure γ rays. The detector is distant and shielded to allow for high beam intensity measurements. More details and examples of the operation of the Super-e can be found in recent papers [28–35].

An 8-MeV proton beam was delivered by the 14UD Pelletron accelerator of HIAF, which was used to excite the 6432-keV 0^+ state of interest in ^{24}Mg through the (p,p′) reaction. The 0_2^+ state is expected to decay via an $E0$ transition to the ground state along with $E2$ transitions to the 2_1^+ and 2_2^+ states. These $E2$ transitions will proceed via γ-ray and electron-positron pair emission, but for the $E0$ transition, only via pair emission. Self-supporting ^{nat}Mg targets were used for the experiment, with thicknesses of $\approx$ 1.8 mg/cm^2. The natural isotopic abundance of ^{24}Mg is 79% with ^{25}Mg and ^{26}Mg present in the target at 10% and 11%, respectively. These contaminants present no significant problem in the analysis. As can be seen in Fig. 2(a) and (b), no transitions from either contaminant are visible in the pair spectrum, and while two transitions are visible from ^{25}Mg in the γ-ray spectrum, they do not complicate the analysis of any of the ^{24}Mg lines of interest.

The target was mounted at 45° to both the beam and the axis of symmetry of the solenoidal bore of the Super-e. This arrangement can be seen on the left-hand side of Fig. 1. Magnesium oxidizes rapidly in the presence of oxygen, and the primary source of background in this experiment was the decay of the 6.050 MeV first-excited 0^+ state in ^{16}O. The targets were freshly prepared shortly before use in order to minimize the ^{16}O contamination.

The magnetic field was operated in a swept-current mode, scanning the solenoid current between 6.2 A–12.25 A in a continuous cyclic fashion. This corresponds to a peak efficiency for electrons and positrons from 1.775–2.885 MeV, and thus pair transition energies from 4.572 MeV to 6.792 MeV. The magnetic field was swept with respect to the integrated beam charge on the beam stop behind the target, giving equal integrated beam current at any given magnetic field value.
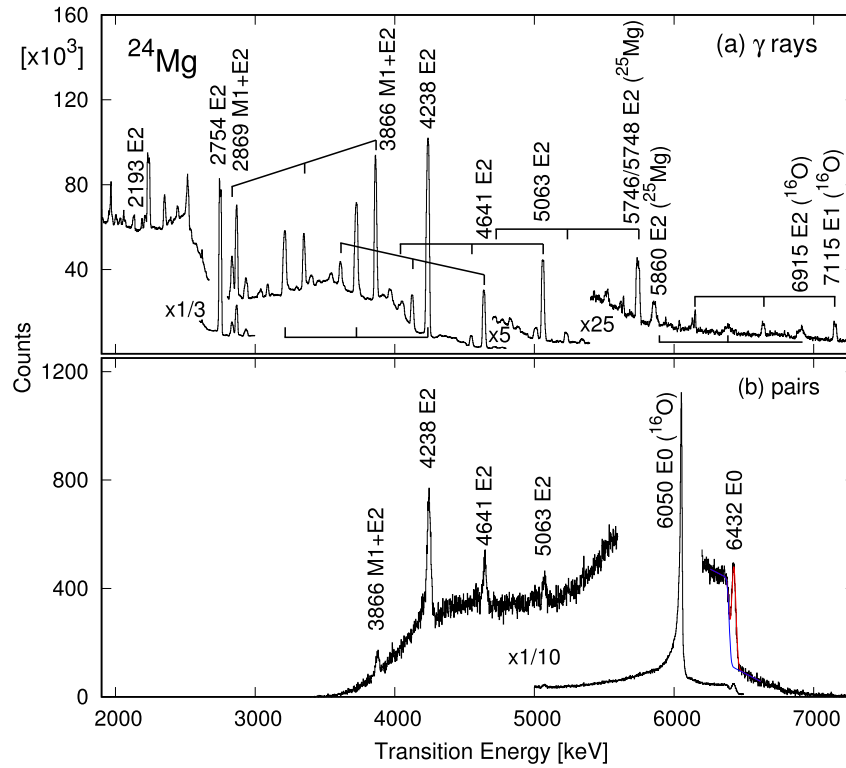
Fig. 2. The (a) γ-ray and (b) electron-positron pair spectra following the ^{24}Mg(p, p') reaction at 8 MeV. In the γ-ray spectrum, the bars demarcate the γ-ray escape peaks, as first escape and second escape. The energies observed in the electron-positron spectrum have been shifted upwards by 1022 keV ($2m_ec^2$) to align with the transition energy. A fit to the 6432-keV $E0$ peak is also shown.

Electron-positron pairs were recorded with *Miel* along with γ-ray singles in the HPGe detector. A beam intensity of $\approx$100 nA as maintained for 106 hours, keeping a total *Miel* singles rate of $\leq$ 10 kHz. The γ rays were recorded to measure the relative intensities of the de-exciting $E2$ transitions, and to normalize the electron-positron pair and γ-ray intensities.

The HPGe relative efficiency was determined using a ^{56}Co source up to 3.451 MeV, and extrapolated to 5.2 MeV. This approach has worked well in previous studies on ^{12}C, ^{40}Ca, and the Fe isotopes [28,29,32,34].

The Super-e pair efficiencies were determined by Monte Carlo simulation. The transmission efficiency of the Super-e was calculated with the use of the LensIpf code [35] with the magnetic field calculated by Poisson Superfish [36]. The detector efficiency for a given electron-positron pair was evaluated using PENELOPE [37] simulations. Further details have been given in Refs. [32,35,38].

The data were stored in an event-by-event format with the energies and times of the six Si(Li) detector segments, the energies of the HPGe γ-ray detectors, and two measures of the magnetic field − the solenoid control voltage and a Hall probe voltage.

There is a strict relationship between the energies and momenta of the transmitted electrons and positrons, and the magnetic field of the solenoid [26,27,32]. A transmission window can be defined as a function of the magnetic field and energy of the charged particles. This momentum selection is used to gate on the data to select out real electron-positron events as a function of their magnetic rigidity [26,32].

The *Miel* detector array has a time resolution of $\approx$10 ns for electrons and positrons of energy greater than 1 MeV. In order to select the true pair events, gates were placed on the time-difference coincidence peak, and the resulting summed energy spectrum was random subtracted by gating on the random time-difference region. The summed electron-positron pair energy spectrum was sorted by combining all 15 possible combinations of *Miel*

Table 1
Experimental results and spectroscopic values used to determine $\rho^2(E0)$.

Quantity	Value	Reference
$I_\gamma^{\text{rel.}}$ (5063 $E2$)	100.0(20)	This work
$I_\gamma^{\text{rel.}}$ (2193 $E2$)	22.2(17)	This work
$I_\pi^{\text{rel.}}$ (6432 $E0$)	0.88(10)	This work
$I_\pi^{\text{rel.}}$ (5063 $E2$)	0.152(14)	This work
τ (6432 0_2^+)	100(10) fs	Evaluated
Ω_π (6432 $E0$)	$1.90(9) \times 10^{11}$ s^{-1}	[47]
α_π (5063 $E2$)	$1.505(21) \times 10^{-3}$	[48]
q_π^2 (6432 $E0$/5063 $E2$)	5.8(8)	This work
X(6432 $E0$/5063 $E2$)	27(4)	This work
ρ^2 (6432 $E0$) $\times 10^3$	380(70)	This work

detector segments while enforcing momentum-selection and time-coincidence conditions.

3. Results

The observed γ-ray spectrum is shown in Fig. 2(a) with the observed electron-positron pair energy spectrum shown in Fig. 2(b). A partial level scheme showing the transitions observed and levels of ^{24}Mg populated in this experiment is shown in Fig. 3. The measured γ-ray relative intensities for the 5063-keV and 2193-keV $E2$ transitions along with the 6432-keV $E0$ and 5063-keV $E2$ internal pair formation relative intensities are given in Table 1.

The value for the $E0$ transition strength depends directly on the state lifetime [4,22]. The lifetime of the 6432-keV 0^+ state has been evaluated from the eight reported lifetimes. These are all Doppler-shift attenuation method measurements, using a variety of reactions [39–45]. The adopted lifetime was determined using the averaging program *AveTools* [46] and *UncTools*, a Monte Carlo statistical analysis tool. The evaluated lifetimes and the new adopted value are shown in Fig. 4. Three lifetime values were excluded from
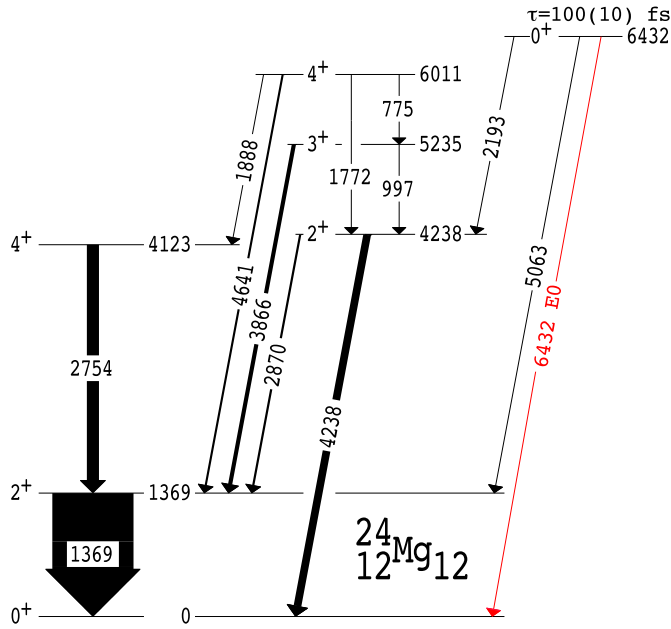
Fig. 3. The level scheme of ^{24}Mg showing the states that were populated in the (p, p') reaction at 8 MeV, and the transitions that were observed. The 4641, 3866, 4238, and 5063 keV transitions were observed in both γ-rays and electron-positron pairs, while the 6432 keV transition was only observed in electron-positron pairs, as expected for an $E0$ transition. See Fig. 2.
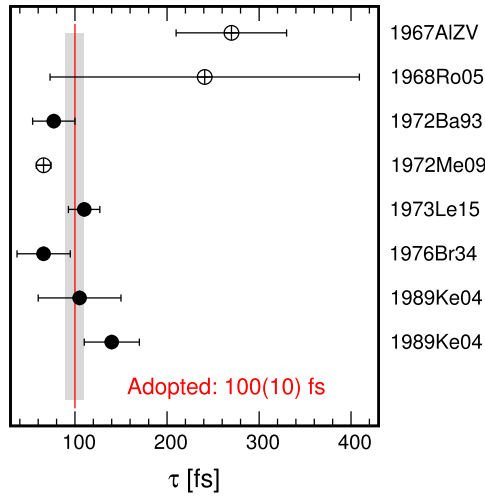

Fig. 4. Plot of mean lifetimes for the 6432-keV 0^+ state in ^{24}Mg. The adopted values used in the lifetime determination are the solid points, and the hollow points are values excluded from the evaluation. The weighted average value of 100(10) fs is shown as a solid red line, with the uncertainty in grey. The data are taken from Refs. [39–45].

the evaluation, one as an outlier [39], one due to the large uncertainty [40], and one for reporting systematically low lifetimes for other states in ^{24}Mg [42].

The new evaluated mean lifetime, and the electronic factor and internal pair formation coefficient, are also given in Table 1. The electronic factor of the 6432-keV $E0$ transition, $\Omega_\pi(6432\ E0)$, is taken from the recent tabulation by Dowie et al. [47] with the adopted 5% relative uncertainty. The pair conversion coefficient for the 5063-keV $E2$ transition, $\alpha_\pi(5063\ E2)$, is taken from the *BrIcc* tables [48].

Using the above values, the $E0/E2$ pair mixing ratio for the 6432-keV $E0$ transition with respect to the 5063-keV $E2$ transition is $q_\pi^2(E0/E2) = 5.8(8)$. The $X(E0/E2)$ value of these transitions — a measure of the relative $E0$ to $E2$ transition strength [49]

— was also determined giving $X(E0/E2) = 27(4)$. Finally, the determined $E0$ strength is: $\rho^2(E0) \times 10^3 = 380(70)$. These results are listed in Table 1. Similarly, the internal pair conversion coefficient for the 4238- and 4641-keV $E2$ transitions have been measured and are $\alpha_\pi(4238\ E2) = 0.00118(11)$, and $\alpha_\pi(4641\ E2) = 0.00124(14)$, compared with the theoretical values of 0.00125(2) and 0.00138(2), respectively [46].

4. Discussion

A value for $\rho^2(E0) \times 10^3$ of 380(70) is very large. It is on par with the largest reported $E0$ strengths in the whole nuclear chart according the most recent evaluation of $E0$ strengths [22] namely: the $E0$ transition strength of the Hoyle state in ^{12}C to the ground state at 500(81) milliunits and the 3633.8-keV $E0$ transition in ^{18}O at 430(80) milliunits. Large $E0$ strengths are a robust indicator of shape coexistence and a clear spectroscopic fingerprint for shape mixing [4]. The $E0$ strength suggests that there is a significant change in the nuclear shape between the first and second 0^+ states and that these states are mixed.

The only previous measurements of the $0_2^+ \rightarrow 0_{\text{g.s.}}^+$ monopole matrix element in ^{24}Mg have been inelastic electron-scattering measurements [23–25]. The previous adopted value for the $E0$ transition strength in ^{24}Mg is 288(11) milliunits [46]. The determination of the monopole matrix element by inelastic electron scattering is model dependent and measurements by direct spectroscopy take priority [22]. Furthermore, concerns have been raised regarding discrepancies between inelastic electron scattering and traditional spectroscopy data [50,51]. Our model-independent experimental result of $\rho^2(E0) \times 10^3 = 380(70)$ has a difference of $\approx 1.3\sigma$ with the previous adopted value of 288(11) milliunits, and thus is consistent within two standard deviations. This measured $E0$ strength supports the statements made by Kibédi and Spear on the general agreement of the $E0$ transition strengths obtained by inelastic electron scattering and more traditional spectroscopy [22,50,51].

One can estimate the $E0$ strength in ^{24}Mg from a simple shell model approach that assumes maximal mixing between oscillator shells, giving $\rho^2(E0) = 0.5A^{-2/3}$, where A is the nuclear mass number [4]. This gives an estimate of $\rho^2(E0) \times 10^3 = 60$, which agrees well with the observed $E0$ $0_2^+ \rightarrow 0_{\text{g.s.}}^+$ strength in ^{26}Mg, but falls short of the observed strength in ^{24}Mg by a factor of six. Brown et al. [52] have developed a more sophisticated approach which combines a configuration interaction model for the valence orbital occupations with an energy-density functional to evaluate the effect of the valence configuration on the core, and hence determine the radial wavefunctions and the $E0$ transition strengths. That model, however, still falls short of the observed $E0$ strengths in sd shell nuclei such as ^{26}Mg and ^{32}S by factors of two to three in the matrix element (or 4 to 9 in the $E0$ transition strengths). The enhanced $E0$ strength in ^{24}Mg therefore suggests a collective explanation such as a significant shape change due to clustering or other excitations outside the sd model space.

Shell model calculations using NuShellX [53] and the USDA interaction [54] in the sd model space for ^{24}Mg also fail to accurately describe the properties of the 0^+ states. The level energies of the positive-parity states with $I \neq 0$ agree closely — within 200–300 keV — with the observed levels, but the 0_2^+ and 0_3^+ states are predicted too high by 1100 and 500 keV, respectively. Furthermore, NuShellX predicts only three 0^+ states below 12 MeV whereas there are four present in the data [55]. The presence of an intruder configuration from outside the model space near the energy of the observed 0_2^+ state, mixing with, and shifting, the expected sd shell-model states, is suggested.

^{24}Mg is well-established as a prolate-deformed nucleus at low excitation energies. The spectroscopic quadrupole moment of the

first 2^+ state is $-0.166(6)$ eb^2 [55], implying, for an axial rotor, a ground-state band β_2 of 0.497(2) (using Eq. (17) from Ref. [56], taking $\beta_4 = 0$ [59,62]). This agrees with experimental determinations of the ground state deformation via inelastic particle scattering [57–62], and theoretical calculations of the ground state deformation [16,63,65,66].

A two-state mixing model (see Section 2.5 in Ref. [4]) is often used to interpret $E0$ strengths in terms of the configuration mixing and difference in intrinsic deformations:

$$\rho^2 = \left(\frac{3Z}{4\pi}\right)^2 a^2 b^2 (\beta_a^2 - \beta_b^2)^2,$$

where a and b are the mixing amplitudes and β_a and β_b are the intrinsic deformations. Taking the limit of maximal mixing ($a = b = 1/\sqrt{2}$) gives $\Delta(\beta^2) \gtrsim 0.43$ for the 0_1^+ and 0_2^+ states of ^{24}Mg, and the change in the mean-square charge radius of the intrinsic configurations is $\Delta\langle r^2 \rangle \gtrsim 1.2$ fm^2. This places a lower limit on the shape change in ^{24}Mg.

However equal mixing of the intrinsic states forming the 0_1^+ and 0_2^+ states in ^{24}Mg is unrealistic. A better (but still approximate) estimate of the mixing between the 0_1^+ and 0_2^+ states can be obtained from the observed excitation energies if an estimate of the unperturbed energy of one of the 0^+ states can be obtained. An estimate of the unperturbed energy of the 0^+ ground state can be obtained by extrapolation to $I = 0$, based on the observed energies of the $I = 2_1^+$, 4_1^+, and 6_1^+ band members. An energy shift of 300–500 keV is implied. Solving the two-state mixing problem for a 500 keV shift gives $a = 0.96$, $b = 0.28$, $\Delta\langle\beta^2\rangle = 0.80$ and $\beta_2(0_2^+) \approx 0.96$. A mean charge radius of the excited state of $\langle r^2 \rangle^{1/2} \approx 3.36$ fm is implied, based on the ground-state mean charge radius from laser spectroscopy [65]. These large deformations suggest that the first-excited 0^+ state in ^{24}Mg could be superdeformed. Similar conclusions are reached for energy shifts less than 500 keV. Furthermore, ^{25}Mg(p, d) transfer reactions [55,64] imply a maximum mixing strength between the two 0^+ states of $b \lesssim 0.41$, which gives $\beta_2(0_2^+) \gtrsim 0.79$ and $\langle r^2 \rangle^{1/2} \gtrsim 3.23$ fm, consistent with the above analysis. Together, these analyses from the energy levels and transfer reactions give evidence that the large $E0$ strength observed in ^{24}Mg arises from a significant shape change between the first-excited 0^+ state and the ground state.

Superdeformation has been found in light nuclei along the $N = Z$ line [1], with superdeformation observed in ^{12}C, ^{16}O, ^{36}Ar, ^{40}Ar, ^{40}Ca, ^{42}Ca, and ^{56}Ni [1,10,11,67–70], and suggested in ^{28}Si [71]. The Nilsson single-particle orbitals, for a β_2 of 1.0, show a superdeformed shell gap at 12 nucleons. This is seen in Fig. 5 where there is a broad gap centred at quadrupole deformation $\beta_2 \approx 0.45$ for 12 nucleons, which could be associated with the ground state, and another pocket at $\beta_2 \approx 1.0$, which could correspond to the first-excited 0^+ state. In the recent review of nuclear shape coexistence by Heyde and Wood [1], a possible shape-coexisting band built on the first-excited 0^+ state in ^{24}Mg was identified with comparable intra-band $B(E2)$ strength to other superdeformed bands in this region; however, much of the spectroscopic information needed to conclusively assign superdeformed character to this state and confirm the presence of the suggested band is missing. The suggested band members were the 7349-keV 2^+ state and the 8439-keV 4^+ state [1]. The $2_{SD}^+ \rightarrow 0_2^+$ transition is unobserved while the $4_{SD}^+ \rightarrow 2_{SD}^+$ has a known $B(E2)$ strength of 39 W.u., corresponding to an estimated $\beta \approx 0.64$ [1,55]. The 8439-keV suggested 4_{SD}^+ band member, however, has a log ft of less than 4 in ^{24}Al β^+ decay, suggesting a $K = 4$ nature, not $K = 0$ [55,72,73]. There is a nearby 9301-keV 4^+ state; this is another possible 4_{SD}^+ band member, which was suggested by Warburton et al. [72] with a similarly large $B(E2)$ strength and estimated β [72]. Future spectroscopy to
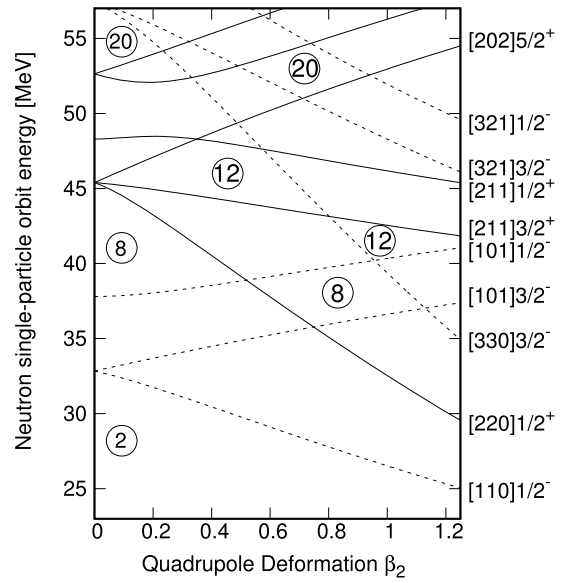

Fig. 5. Plot of neutron single-particle energies as a function of the quadrupole deformation parameter β_2. The solid and dashed lines are for positive and negative parity orbitals, respectively. The two deformed shell-gaps corresponding to 12 nucleons are shown in the plot, along with the deformed shell gaps at 8 and 20 nucleons. The typical spherical shell-gaps at 2, 8, and 20 are also shown. The parameters used for the calculation are found in Ref. [74] and β_4 is taken as 0 [59,62]. Similar behaviour is observed for the proton single-particle energies.

resolve quadrupole moments and state lifetimes is needed to resolve these issues and determine the nature of these states and possible superdeformation.

There has been ongoing theoretical effort devoted to investigating the structure of ^{24}Mg in terms of cluster dynamics [14–16,66]. Theoretical work on ^{24}Mg looking into the structure of excited 0^+ states, in particular using antisymmetrized molecular dynamics combined with the generator coordinate method and the Gogny D1S interaction, has been carried out by Chiba and Kimura [16]. They determine that the lower-lying excited 0^+ states (excitation energy <15 MeV) are strong mixtures of mean-field and ^{20}Ne $+ \alpha$ and ^{12}C $+^{12}$C cluster configurations. In particular, the first-excited 0^+ state, which they identify with the experimental 6432-keV 0^+ state investigated here, is predominantly a mixture of a mean-field configuration with large deformation — $(\beta, \gamma) = (0.76, 35°)$ — and the ^{20}Ne $+ \alpha$ cluster configuration. Likewise, they identify the ground state as a mixture of a less deformed configuration — $(\beta, \gamma) = (0.48, 22°)$ — along with the ^{20}Ne $+ \alpha$ and ^{12}C $+^{12}$C cluster configurations. This seems to be in agreement with the results of the present work, which indicate a significant increase in deformation between the two 0^+ states.

Recent work on shape isomerism in light, alpha-conjugate nuclei (^{16}O, ^{20}Ne, ^{24}Mg) through a self-consistent analysis of the quasi-dynamical SU(3) symmetry also predicts a shape-coexisting state in ^{24}Mg with a Nilsson quadrupole deformation of $\epsilon = 0.91$, equivalent to $|\beta_2| \approx 1.0$, for a wide range of triaxiality [75]. These results are concordant with the experimental estimate of $|\beta_2| \approx 1$ and the picture of superdeformation in the deformed shell gap shown in Fig. 5, which is also in agreement with the Nilsson-model and α-cluster calculations [76–79].

5. Conclusion

The first direct observation of the $E0$ transition from the first-excited 0^+ state in ^{24}Mg to the ground state has been reported. Through electron-positron pair spectroscopy, the 6432-keV $E0$ transition was observed, its intensity measured, and by adopting a lifetime of $\tau = 100(10)$ fs from the literature, the $E0$ transition

strength was determined to be $\rho^2(E0) \times 10^3 = 380(70)$. Estimates of the deformation and mean-square charge radius of the excited 0^+ state give a $|\beta_2|(0_2^+) \approx 1$ and $\langle r^2 \rangle^{1/2} \approx 3.36$ fm. These results reveal shape mixing and significant shape change between the ground state and the first-excited 0^+ state. Indeed, with an estimated $|\beta_2|$ of 1, the first-excited 0^+ state appears to be superdeformed. Spectroscopic information needed to firmly identify the excited superdeformed band — such as $E2$ transition strengths — is lacking and this deficiency should be rectified at the first opportunity. Recent theoretical calculations of the structure of ^{24}Mg suggest mixing and significant shape change between the ground-state and first-excited 0^+ state, both of which are supported by the present results.

Declaration of competing interest

References

[1] K. Heyde, J.L. Wood, Rev. Mod. Phys. 83 (2011) 1467.
[2] M. Freer, Rep. Prog. Phys. 70 (2007) 2149.
[3] D.G. Jenkins, J. Phys. G, Nucl. Part. Phys. 43 (2016) 024003.
[4] J.L. Wood, E.F. Zganjar, C. De Coster, K. Heyde, Nucl. Phys. A 651 (1999) 323.
[5] D.G. Jenkins, S. Courtin, J. Phys. G, Nucl. Part. Phys. 42 (2015) 034010.
[6] E.E. Salpeter, Astrophys. J. 115 (1952) 326.
[7] F. Hoyle, Astrophys. J. Suppl. Ser. 1 (1954) 121.
[8] M. Chernykh, H. Feldmeier, T. Neff, P. von Neumann-Cosel, A. Richter, Phys. Rev. Lett. 98 (2007) 032501.
[9] E. Epelbaum, H. Krebs, D. Lee, U.-G. Meissner, Phys. Rev. Lett. 106 (2011) 192501.
[10] E. Ideguchi, et al., Phys. Rev. Lett. 87 (2001) 222501.
[11] E. Ideguchi, et al., Phys. Lett. B 686 (2010) 18.
[12] E. Caurier, J. Menéndez, F. Nowacki, A. Poves, Phys. Rev. C 75 (2007) 054317.
[13] A.G.W. Cameron, Stellar Evolution, Nuclear Astrophysics, and Nucleogenesis, Dover Publications, New York, 2013.
[14] R.A. Baldock, B. Buck, J. Phys. G, Nucl. Phys. 12 (1986) L29.
[15] P. Descouvemont, Nucl. Phys. A 709 (2002) 275.
[16] Y. Chiba, M. Kimura, Phys. Rev. C 91 (2015) 061302(R).
[17] E. Almqvist, D.A. Bromley, J.A. Kuehner, Phys. Rev. Lett. 4 (1960) 515.
[18] D.A. Bromley, J.A. Kuehner, E. Almqvist, Phys. Rev. Lett. 4 (1960) 365.
[19] C.L. Jiang, B.B. Back, H. Esbensen, R.V.F. Janssens, K.E. Rehm, R.J. Charity, Phys. Rev. Lett. 110 (2013) 072701.
[20] G. Fruet, et al., Phys. Rev. Lett. 124 (2020) 192701.
[21] W.P. Tan, et al., Phys. Rev. Lett. 124 (2020) 192702.
[22] T. Kibédi, R.H. Spear, At. Data Nucl. Data Tables 89 (2005) 77.
[23] O. Titze, Z. Phys. 220 (1969) 66.
[24] P. Strehl, Z. Phys. 234 (1970) 416.
[25] A. Johnston, T.E. Drake, J. Phys. A 7 (1974) 898.
[26] T. Kibédi, G.D. Dracoulis, A.P. Byrne, Nucl. Instrum. Methods Phys. Res., Sect. A 294 (1990) 523.
[27] T. Kibédi, M. Kerr, E.B. Norman, G.D. Dracoulis, A.P. Byrne, Astrophys. J. 489 (1997) 591.
[28] T.K. Eriksen, et al., JPS Conf. Proc. 14 (2017) 020404.
[29] T.K. Eriksen, et al., Proc. Sci. 281 (2017) 069.
[30] L.J. Evitts, et al., Phys. Lett. B 779 (2018) 396.
[31] L.J. Evitts, et al., Phys. Rev. C 99 (2019) 024306.
[32] T.K. Eriksen, et al., Phys. Rev. C 102 (2020) 024320.
[33] J.T.H. Dowie, et al., EPJ Web Conf. 232 (2020) 04004.
[34] E. Ideguchi, et al., in preparation.
[35] T. Kibédi, T.K. Eriksen, J.T.H. Dowie, T. Tunningley, A.E. Stuchbery, in preparation.
[36] K. Halbach, R.F. Holsinger, Part. Accel. 7 (1976) 213.
[37] F. Salvat, J.M. Fernández-Varea, J. Sempau (Eds.), PENELOPE-2008: A Code System for Monte Carlo Simulation of Electron and Photon Transport, Workshop Proceedings, Barcelona, Spain, 30 June-3 July 2008.
[38] T.K. Eriksen, PhD Thesis, ANU, 2018.
[39] T.K. Alexander, et al., in: Int. Nucl. Phys. Conf., Gatlinburg, Tenn., 1966, Academic Press, New York, 1967, p. 367.
[40] S.W. Robinson, R.D. Bent, Phys. Rev. 168 (1968) 1266.
[41] S.I. Baker, C.R. Gossett, P.A. Treado, J.M. Lambert, L.A. Beach, Nucl. Phys. A 196 (1972) 197.
[42] M.A. Meyer, J.P.L. Reinecke, D. Reitmann, Nucl. Phys. A 185 (1972) 625.
[43] F. Leccia, M.M. Aléonard, D. Castéra, Ph. Hubert, P. Mennrath, J. Phys. 34 (1973) 147.
[44] D. Branford, L.E. Carlson, F.C.P. Huang, N. Gardner, T.R. Ophel, I.F. Wright, Aust. J. Phys. 29 (1976) 139.
[45] J. Keinonen, P. Tikkanen, A. Kuronen, Á.Z. Kiss, E. Somojai, B.H. Wildenthal, Nucl. Phys. A 493 (1989) 124.
[46] T. Kibédi, AveTools v3.0, 10-DEC-2014, https://www-nds.iaea.org/public/ensdf_pgm/.
[47] J.T.H. Dowie, T. Kibédi, T.K. Eriksen, A.E. Stuchbery, At. Data Nucl. Data Tables 131 (2020) 101283.
[48] T. Kibédi, T.W. Burrows, M.B. Trzhaskovskaya, P.M. Davidson, C.W. Nestor Jr., Nucl. Instrum. Methods A 589 (2008) 202.
[49] J.O. Rasmussen, Nucl. Phys. 19 (1960) 85.
[50] P.M. Endt, At. Data Nucl. Data Tables 23 (1979) 3.
[51] P.M. Endt, At. Data Nucl. Data Tables 55 (1993) 171.
[52] B.A. Brown, A.B. Garnsworthy, T. Kibédi, A.E. Stuchbery, Phys. Rev. C 95 (2017) 011301(R).
[53] B.A. Brown, W.D.M. Rae, Nucl. Data Sheets 120 (2014) 115.
[54] W.A. Richter, S. Mikhize, B.A. Brown, Phys. Rev. C 78 (2008) 064302.
[55] R.B. Firestone, Nucl. Data Sheets 108 (2007) 2319.
[56] S. Raman, C.W. Nestor Jr., P. Tikkanen, At. Data Nucl. Data Tables 78 (2001) 1.
[57] H. Rebel, G.W. Schweimer, G. Schatz, J. Specht, R. Löken, G. Hauser, D. Habs, H. Klewe-Nebenius, Nucl. Phys. A 182 (1972) 145.
[58] J. Eenmaa, R.K. Cole, C.N. Waddell, H.S. Sandhu, R.R. Dittman, Nucl. Phys. A 218 (1974) 125.
[59] G. Haouat, Ch. Lagrange, R. de Swiniarski, F. Dietrich, J.P. Delaroche, Y. Patin, Phys. Rev. C 30 (1984) 1795.
[60] S. Kato, et al., Phys. Rev. C 31 (1985) 1616.
[61] D.C. Hensley, E.E. Gross, M.L. Halbert, J.R. Beene, F.E. Bertrand, G. Vourvopoulos, D.L. Humphrey, T. VanCleve, Phys. Rev. C 40 (1989) 2065.
[62] R. de Swiniarski, D.L. Pham, J. Raynal, Z. Phys. A 343 (1992) 179.
[63] N. Hinohara, Y. Kanada-En'yo, Phys. Rev. C 83 (2011) 014321.
[64] R.C. Haight, PhD Thesis, Princeton Univ., 1969.
[65] D.T. Yordanov, et al., Phys. Rev. Lett. 108 (2012) 042504.
[66] M. Kimura, R. Yoshida, M. Isaka, Prog. Theor. Phys. 127 (2012) 287.
[67] D. Rudolph, et al., Phys. Rev. Lett. 82 (1999) 3763.
[68] K. Hadyńska-Klȩk, et al., Phys. Rev. Lett. 117 (2016) 062501.
[69] K. Hadyńska-Klȩk, et al., Phys. Rev. C 97 (2018) 024326.
[70] C.E. Svensson, et al., Phys. Rev. Lett. 85 (2000) 2693.
[71] D.G. Jenkins, Phys. Rev. C 86 (2012) 064308.
[72] E.K. Warburton, C.J. Lister, D.E. Alburger, J.W. Olness, Phys. Rev. C 23 (1981) 1242.
[73] J. Honkanen, M. Kortelahti, K. Ayesto, A. Eskola, A. Hautojarvi, Phys. Scr. 19 (1979) 239.
[74] T. Bengtsson, I. Ragnarsson, Nucl. Phys. A 436 (1985) 14.
[75] J. Cseh, G. Riczu, J. Darai, Phys. Lett. B 795 (2019) 160.
[76] G. Leander, S.E. Larsson, Nucl. Phys. A 239 (1975) 93.
[77] A.C. Merchant, W.D.M. Rae, Nucl. Phys. A 549 (1992) 431.
[78] J. Zhang, W.D.M. Rae, Nucl. Phys. A 564 (1993) 252.
[79] J. Zhang, W.D.M. Rae, A.C. Merchant, Nucl. Phys. A 575 (1994) 61.